KERNFORSCHUNGSZENTRUM KARLSRUHE

Dezember 1964 KFK 262

Institut für Angewandte Kernphysik

The Phonon Frequency Distribution of Vanadium

W. Gläser, F. Carvalho, G. Ehret

GESELLSCHAFT FÜR KERNFORSCHUNG M. B. H.
KARLSRUHE

Gesellschaft für Kernforschung m.b.H.

Karlsruhe

KERNFORSCHUNGSZENTRUM KARLSRUHE

December 1964 K F K 262

Institut für Angewandte Kernphysik

The Phonon Frequency Distribution of Vanadium

by

W. Gläser, F. Carvalho*, and G. Ehret

A paper submitted to the IAEA Symposium on the Inelastic Scattering of Neutrons
Bombay, India, 15 - 19 December 1964

*On leave of absence from Junta de Energia Nuclear, Portugal

Gesellschaft für Kernforschung m.b.H., Karlsruhe

I. Introduction

The investigation of inelastic scattering of slow neutrons in solids yields valuable information on the dynamic properties of such many-particle systems. If the coherent scattering is dominant, single phonons can be "seen" and, as a result of systematic measurements of phonons in certain directions in single crystals, dispersion curves can be constructed. If the scattering is incoherent, this method is not possible. In this case, however, the frequency distribution of the normal modes can be deduced in a more or less direct way from the measured scattering distribution. Comparison of experimental and theoretical frequency distributions often suggests a more realistic picture of the properties of the scatterer. Unfortunately, only a few substances scatter almost completely incoherently. From these, vanadium, with a cubic body centered lattice, has a relative simple structure. Several workers [1 - 4] have reported frequency distributions of vanadium obtained by the scattering of beryllium filtered cold neutrons. In the present paper, a somewhat different method is described in which the scattering law of vanadium is measured for a relatively large range of momentum transfer, $\hbar Q$, and energy transfer, $\hbar \omega$ ($0 < Q < 14$ Å^{-1}; $0 < \hbar\omega < 2k_B T$). Starting with the scattering law values and using the extrapolation technique proposed by Egelstaff [5], values of the frequency distribution function have been obtained. The only assumption made for the purpose of performing the iteration of the extrapolated values is that the motions of the atoms are harmonic. But then the separation of multi-phonon processes is straightforward and no previous evaluation of the Debye-Waller factor is necessary.

II. Experimental Arrangement and Procedure

A beam from the Karlsruhe rotating-crystal time-of-flight spectrometer described earlier in detail [6] provided the incident monoenergetic neutrons in an energy range of 18 to 80 meV. Primary energy resolution was 5 % at 18 meV and time resolution about 20 μsec/m.

A sketch of the apparatus is shown in Fig. 1. The distance sample--detector was 2 m. Nine detectors at scattering angles between 20 and 140° were used simultaneously. At present, two different types of

detectors are in use, namely He^3-counters, 1 inch diameter, forming banks with an effective area of 155 cm^2, and Li^6F-ZnS scintillators, 5 inch in diameter. For data acquisition and reduction, a multiple input data acquisition system (MIDAS) with a Control Data 160-A computer (8K core memory) as central unit is employed /7/. This computer handles simultaneously on-line four different reactor beam experiments. The events recorded by the time-of-flight detectors of the scattering experiment are fed into a multiparameter coding unit which digitizes the experiment number, the particular detector number and the neutron time-of-flight. This unit is connected with the computer by means of a central buffer station.

The scattering sample was a 7 x 4.5 cm^2 vanadium plate with a thickness of 0.2 cm. The transmission of the sample was 85 % for incident neutrons of the smallest energy and about 90 % for the highest energy used. For each of the three incident energies (about 18, 40 and 80 meV) a run of approximately 50 hours duration was carried out. This corresponds to a few hundred counts in the significant inelastic channels. For background elimination similar runs without the sample were made. Because of the rotational symmetry of the crystal monochromator, background contributions from fast neutrons and uncorrelated slow neutrons are constant in time and are, therefore, easily corrected.

III. Data Processing and Results

The quantity to be directly calculated from the measured scattering distributions is the scattering law $S(\alpha,\beta)$, defined as follows:

$$S(\alpha,\beta) = \frac{4\pi k_B T}{\sigma_f} \left(\frac{A}{A+1}\right)^2 e^{\beta/2} \left(\frac{E_o}{E}\right)^{1/2} \frac{d^2\sigma}{d\Omega dE} \qquad (1)$$

where

$\frac{d^2\sigma}{d\Omega dE}$ is the double differential neutron scattering cross-section,

σ_f the free atom cross-section of the scattering nucleus,

k_B the Boltzmann constant,

T the absolute temperature of the scatterer,

A the ratio of the mass of the scattering nucleus to the mass of the neutron,

$d\Omega$ the element of solid angle into which the neutrons are scattered,

E_o and E the incident and scattered neutron energies,

$$\beta = \frac{E - E_o}{k_B T} \quad , \tag{2}$$

$$\alpha = \frac{E_o + E - 2\,(E_o E)^{1/2} \cos\theta}{A k_B T} \tag{3}$$

and θ the scattering angle.

For incoherently scattering solids a direct relation can be established, in the harmonic approximation, between the phonon frequency distribution of the crystal lattice $\rho(\beta)$ and the limiting value of $S(\alpha,\beta)/\alpha$ for $\alpha = 0$:

$$\rho(\beta) = 2\beta \sinh \beta/2 \quad (S/\alpha)_{\alpha=0} \tag{4}$$

In a first step a "callibration program" was run for the purpose of calculating the detector efficiency as a function of energy. Here effects of sample thickness, mainly absorption, are taken into account. The calculation is based on the Placzek heavy-mass expansion [8]. A function of the type proposed by Harris et al. [9] has been fitted to the calculated efficiency values. The resulting parameters were fed into the computer together with the raw data from sample-in and sample-out runs and a second calculation was started with the "scattering law program", which delivers the α, β, $S(\alpha,\beta)$, $S(\alpha,\beta)/\alpha$ and the statistical errors of the measurement for each time channel. In this program the built-in possibility of smoothing the raw-data in selected time-channel intervals has been taken to advantage when advisable, namely for the background data and the sample-in data at the lowest energy. A typical result for $S(\alpha,\beta)/\alpha$ vs. time-channel is shown in Fig. 2.

The calculated $S(\alpha,\beta)/\alpha$ values are then plotted against α and extrapolated to $\alpha = 0$ for β values at 0.05 intervals (Fig. 3). In the first extrapolation the resolution effects that tend to increase the gradient of the S/α curves, especially at low α, have not been corrected for. Then the LEAP program [10] has been run with those first exprapolated values, assuming that the gradient of the LEAP output curves would be approximately correct. Based on this gradient a correction for the elastic peak resolution was

performed using the assumption that the peak shape and also the energy resolution for a given time-channel and a given incident energy are independent of the scattering angle.

It was further assumed that the α-dependence of the elastic amplitude in a given channel is described by the Debye-Waller factor. This resolution correction determines a parallel displacement of the curves calculated with LEAP which is of significance only for low ß values.

With the new extrapolated values a second LEAP calculation was made and the results were again compared with the measured data; this procedure was repeated until the slope of the L-lines (Fig.3) and their limit at $\alpha = 0$ stabilized themselves. Three runs were made, $\rho(ß)$ being normalized to one at every run. The variations of the calculated Debye-Waller factor and of the area under the input-$\rho(ß)$ during the whole process were not greater than 10 %. Figs. 4 and 5 show the obtained $(S/\alpha)_{\alpha = 0}$ and $\rho(ß)$ curves.

IV. Discussion of results

In Fig. 6 the final frequency distribution $\rho(\nu)$ extracted from the scattering law measurements is compared with some of the previously reported measurements using the beryllium-filter technique. The area under each curve is normalized to unity. Roughly all of them show the same shape but in details there are disagreements. The curve 3 is corrected for the distribution of the incident neutrons [3]. The decrease in peak height in our curve may be partially due to some extra scattering at higher energies; a decrease may be caused also by resolution effects in the inelastic spectrum. But another possible explanation is the effect of multiple scattering; in our measurements we used much thinner samples than the other workers did.

The present curve has a small bump at $\nu = 2{\cdot}4{\cdot}10^{12}$ sec^{-1}. The existence of such a peak has been predicted previously at about $\nu = 2{\cdot}10^{12}$ sec^{-1} and attributed to the Kohn effect [11].

Although vanadium has a high transition temperature for the super-conducting state indicating a strong electron-phonon interaction which favours a strong Kohn effect, such a peak, in principle, can be expected also on the basis of Born-von Kármán-theory. Using a

a model with noncentral nearest neighbour and central next neighbour interaction Singh and Bowers [12] calculated a frequency spectrum showing three peaks. Unfortunately they did not use the correct elastic constants. After the elastic constants of vanadium had been measured by Alers [13], calculations using the Born-von Kármán and the de Launay models have been made [14]. None of the models, however, gives a satisfactory representation of the measured frequency distributions.

From the LEAP calculations the Debye-Waller coefficient $\lambda = 2\ W/\alpha$ is found to be $4.22 \pm 10\ \%$. In the Debye approximation a Debye temperature $\Theta_0 = 354 \pm 15^{\circ}K$ can be deduced from this value. Starting from the measured frequency distribution we calculated the specific heat as a function of temperature. The results are well described by the above Debye temperature and are, within the experimental errors, in agreement with the low temperature specific heat measurements by Corak et al. [15].

Acknowledgements

The authors wish to thank Prof. K. H. Beckurts who has initiated the inelastic neutron scattering work in our laboratory for his continuing support. Dr. P. A. Egelstaff (Harwell) has made the LEAP program available prior to publication. Thanks for invaluable technical assistance are due to Dipl.-Ing. H. Ripfel, H. D. Jünger and the staff of the Karlsruhe IBM 7070.

References

[1] Stewart, A. T. and Brockhouse, B. N., Rev. Mod. Phys. 30 (1958), 250.

[2] Eisenhauer, C. M., et al., Phys. Rev. 109 (1958), 1046.

[3] Semljanov, M. G., et al., "Inelastic Scattering of Neutrons in Solids and Liquids", Vol. II, IAEA, Vienna (1963), 125.

[4] Haas, R. et al., "Inelastic Scattering of Neutrons in Solids and Liquids", Vol. II, IAEA, Vienna (1963) 145.

[5] Egelstaff, P. A., "Inelastic Scattering of Neutrons in Solids and Liquids", IAEA, Vienna (1961) 25.

[6] Carvalho, F. et al., Study Group Meeting on Research Reactor Experimental Techniques, Bucharest, October 26 - 31, (1964).

[7] Krüger, G. and Dimmler G., Proc. EANDC Conf. on the Automatic Acquisition and Reduction of Nucl. Data, Karlsruhe (1964) 149.

[8] Placzek, G., Phys. Rev. 86 (1952) 377.

[9] Harris, D., Duffil, C., "Inelastic Scattering of Neutrons in Solids and Liquids", Vol. I, IAEA, Vienna (1963) 171.

[10] Mc Latchie, R., Program description LEAP, AERE Harwell (1962).

[11] Pelah, I., "Inelastic Scattering of Neutrons in Solids and Liquids", Vol. II, IAEA, Vienna (1963) 155.

[12] Singh, D. N. and Bowers, W. A., Phys. Rev. 116 (1959) 279.

[13] Alers, G. A., Phys. Rev. 119 (1960) 1532.

[14] Hendricks, J. B., Phys. Rev. 130 (1963) 1377.

[15] Corak, W. S. et al., Phys. Rev. 102 (1956) 656.

Legends to figures:

Fig. 1: Schematic sketch of the rotating-crystal time-of-flight spectrometer at the FR2 reactor.

Fig. 2: Typical plot of $S(\alpha,\beta)/\alpha$ values obtained with the "scattering-law program"

Fig. 3: Typical curves of log (S/α) vs. α; L indicates the curves from the final LEAP calculation; R 80 and R 40 the curves calculated on the basis of L and the resolution correction sketched in the text, for incident energies of 80 and 40 meV.

Fig. 4: The values of $(S/\alpha)_{\alpha = 0}$ vs. β.

Fig. 5: $\rho(\beta)$ deduced from the measurements.

Fig. 6: A comparison of several experimental frequency distributions for vanadium. The number on the curve gives the reference.
Curve 4 is the result of the present work.

FIG. 1

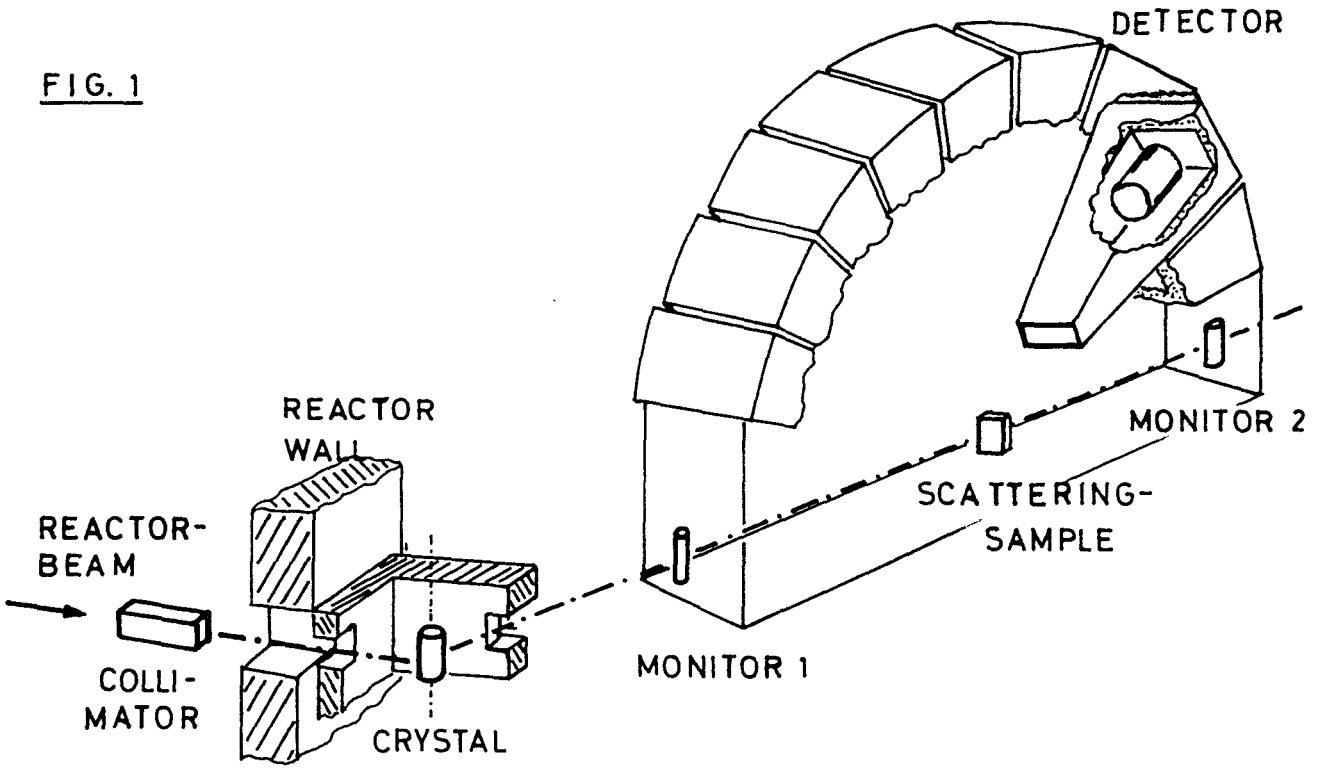

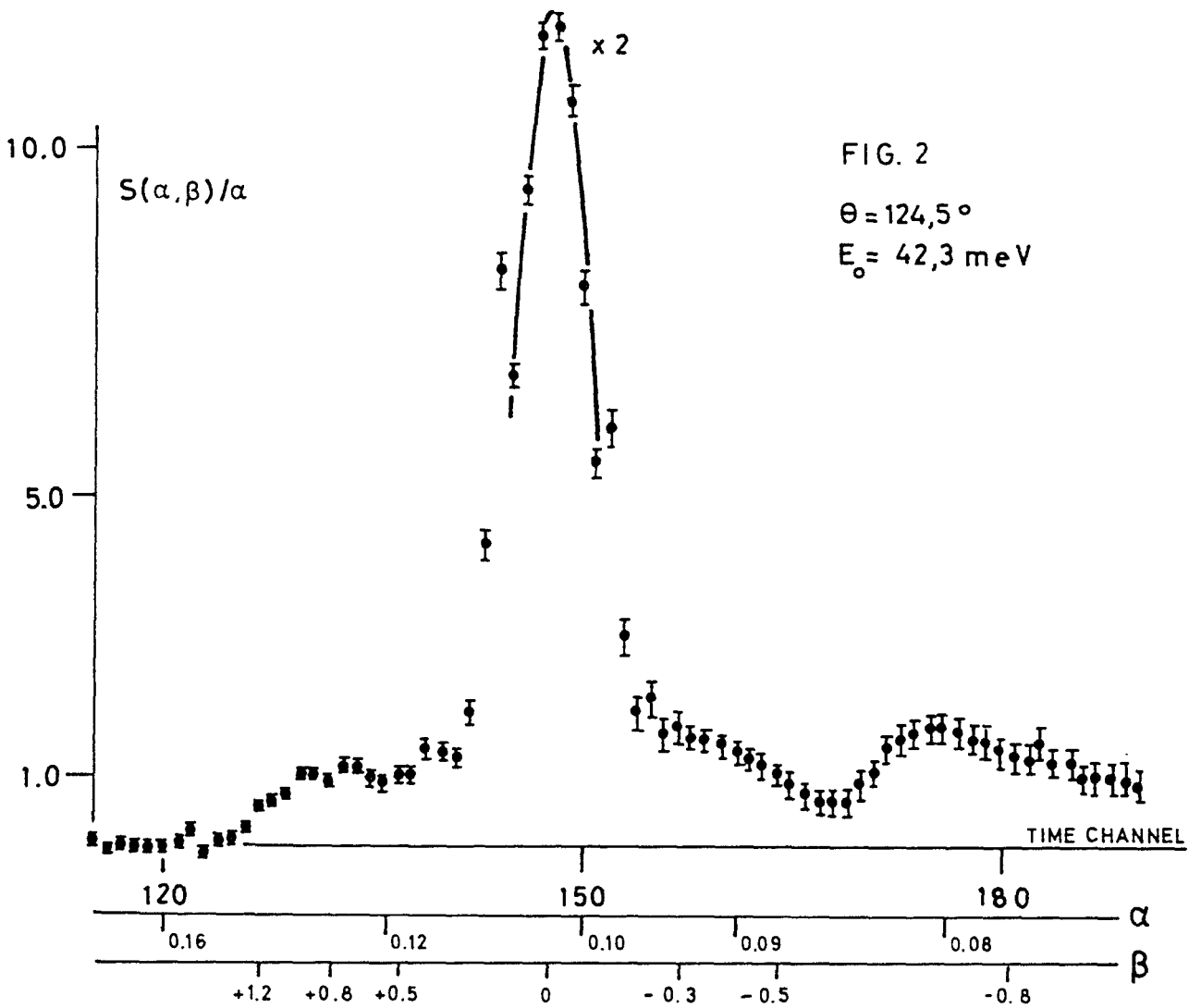

FIG. 2

$\theta = 124{,}5°$

$E_o = 42{,}3$ meV

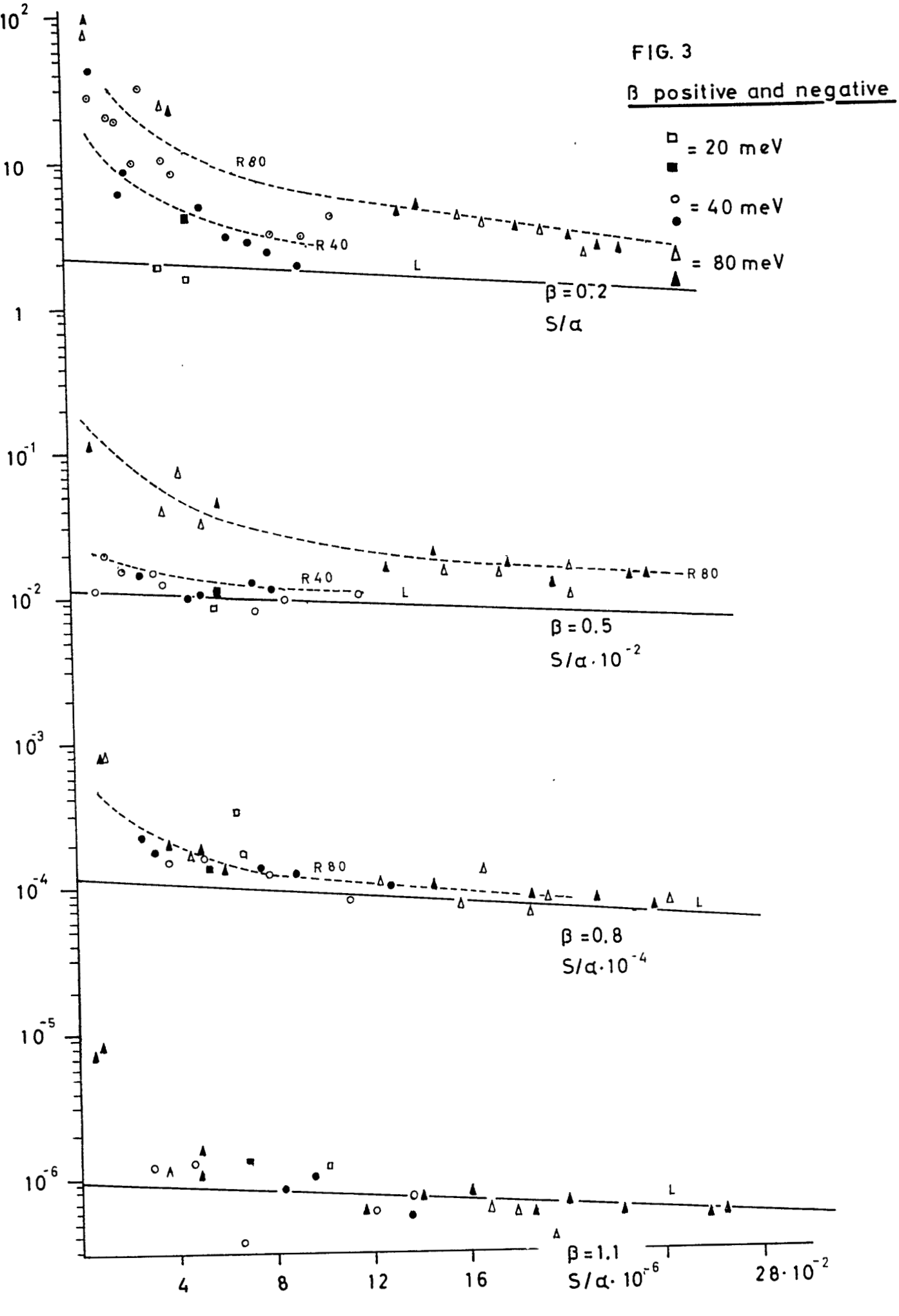
FIG. 3
β positive and negative
= 20 meV
= 40 meV
= 80 meV
R 80
R 40
L
β = 0.2
S/α
β = 0.5
S/α · 10^-2
β = 0.8
S/α · 10^-4
β = 1.1
S/α · 10^-6
10^2
10
1
10^-1
10^-2
10^-3
10^-4
10^-5
10^-6
4
8
12
16
28 · 10^-2
α

FIG. 4

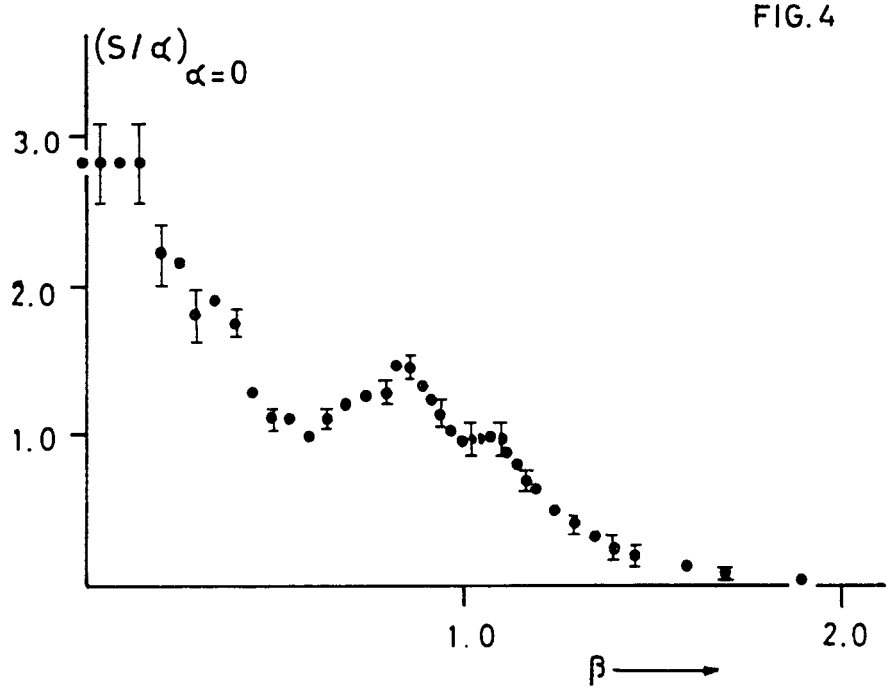

FIG. 5

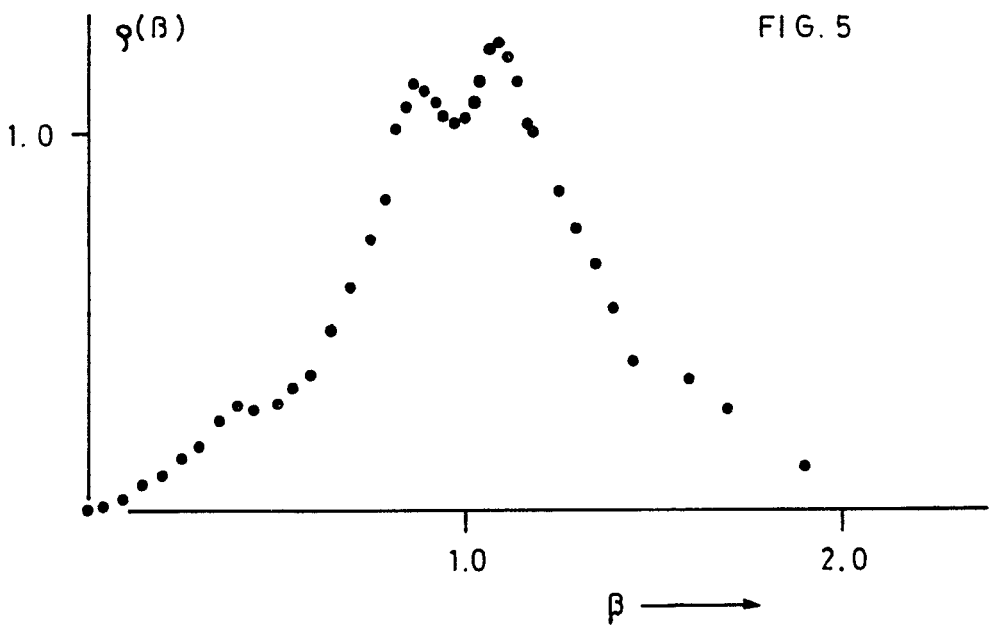

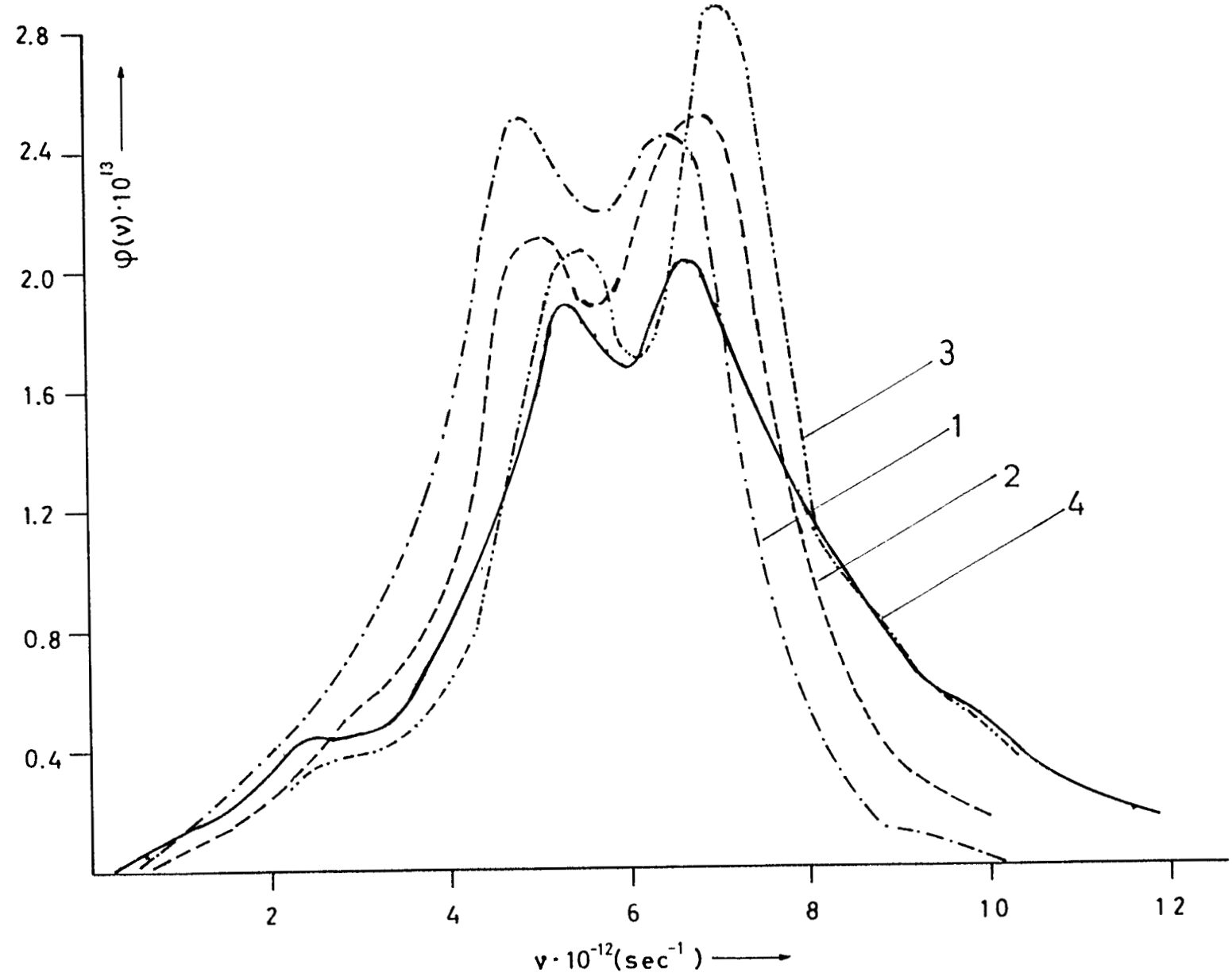

FIG. 6